

Robust Data Fusion for Cooperative Vehicular Localization in Tunnels

Gia-Minh Hoang^{1,2}, Benoît Denis¹, Jérôme Härrri² and Dirk T.M. Slock²

Abstract—In an effort to improve positioning accuracy in Vehicular Ad hoc NETWORKS (VANETs), Cooperative Localization (CLoc) has been proposed to fuse *relative* observations from Vehicle-to-Vehicle (V2V) communication devices with *absolute* observations from on-board resources such as Global Navigation Satellite Systems (GNSS), Inertial Measurement Units (IMU), and Wheel Speed Sensors (WSSs). In challenging but common tunnel environments, prolonged GNSS outages and unsustainable error accumulation of inertial sensors over time (e.g., gyroscopes) lead to the fast divergence of position estimates. In this paper, we aim at resolving this problem by relying on additional Vehicle-to-Infrastructure (V2I) measurements, making use of RoadSide Units (RSUs) internally to the tunnel. In particular, we explore practical trade-offs between V2I technology (i.e., Impulse Radio - Ultra WideBand (IR-UWB) or ITS-G5) and RSUs deployment costs (i.e., in terms of density and geometric configuration), while improving CLoc *absolute* accuracy. We also consider combining this solution with lane detection capabilities (e.g., camera-based) and associated road information, while comparing it with a more conventional approach based on GNSS repeaters.

I. INTRODUCTION

Future Cooperative Intelligent Transport Systems (C-ITS) applications based on Vehicular Ad hoc NETWORKS (VANETs) assume the availability of a positioning system to provide each vehicle with accurate location information regardless of operating conditions. Although the Global Navigation Satellite System (GNSS) is the most common, accessible and obvious choice for vehicle localization today, it still fails to fulfill C-ITS application requirements, especially in challenged environments such as long tunnels and dense urban canyons. In this context, Cooperative Localization (CLoc), which takes advantage of ubiquitous location awareness through Vehicle-to-Vehicle (V2V) communications, appears as a promising complementary strategy. Contextually, an “ego” vehicle considers its neighbors as potential “virtual anchors” [1]–[4] (i.e., mobile anchors with imperfect location information). CLoc is organized in three phases. First, each vehicle encapsulates its latest *absolute*

location in a Beacon¹ broadcast over V2V communication links. After receiving such Beacons, a given “ego” vehicle becomes aware of the estimated *absolute* positions of its neighbors. The second phase aims at retrieving *relative* V2V location-dependent information with respect to the “virtual anchors”, either directly out of received Beacon signals (e.g., based on physical radiolocation metrics) or by relying on a side ranging-enabled wireless technology. All this cooperative information (i.e., V2V measurements and claimed neighbors’ estimates) is then combined with the locally predicted “ego” position based on on-board devices, such as an Inertial Measurement Unit (IMU), a Wheel Speed Sensor (WSS), and whenever available, a GNSS receiver. Hybrid data fusion techniques are then applied to further refine the “ego” *absolute* position accordingly (See Fig. 1). In the last phase, the “ego” vehicle contributes to improve also the localization of other vehicles by sharing its own fusion-based position estimates in subsequent Beacons.

V2V communications have stimulated research interest in the field of CLoc for the last past years, making it possible to exploit signals of opportunity such as the Received Signal Strength Indicators (RSSIs) of received Cooperative Awareness Messages (CAMs) [1], [3]–[5], in compliance with Vehicle-to-X (V2X) ITS-G5 technology [6]². For the sake of improving further localization performances, in [7], [8], ITS-G5-based RSSI measurements are replaced by Impulse Radio - Ultra WideBand (IR-UWB) Time-of-Flight (ToF) measurements (See Fig. 1), which can theoretically performed within centimeter-level distance resolutions [9]. However, despite fine V2V ranging accuracy, in large-scale GNSS-denied environments like long tunnels, performing CLoc over large time periods with respect to “virtual anchors” only is subject to divergence issues. This is due to errors propagation through cooperation in lack of absolute re-calibration means (e.g., re-injecting unbounded biased neighbors’ positions from vehicle to vehicle) and/or poor Geometric Dilution of Precision (GDoP) constrained by both vehicular mobility and road width. Alternatively, in such pathological environments, conventional (non-cooperative) GNSS-based solutions based on a high density of repeaters in the tunnel (e.g., typically, one every 30–50 meters) are notoriously costly and necessitate huge deployment efforts to retrieve just the nominal clear-sky GNSS accuracy (at most, in optimistic cases).

In this paper, we thus propose a new CLoc scheme mixing

This work has been performed in the frame of the *HIGHTS* project, which is funded by the European Commission (636537-H2020). EURECOM acknowledges the support of its industrial members, namely, BMW Group, IABG, Monaco Telecom, Orange, SAP, ST Microelectronics, and Symantec.

^{1,2}Gia-Minh Hoang is with CEA-Leti, MINATEC Campus, 17 avenue des Martyrs, 38054 Grenoble, France, and also with EURECOM, SophiaTech Campus, 450 route des Chappes, 06904 Biot, France giaminh.hoang@cea.fr

¹Benoît Denis is with CEA-Leti, MINATEC Campus, 17 avenue des Martyrs, 38054 Grenoble, France benoit.denis@cea.fr

²Jérôme Härrri and Dirk T.M. Slock are with EURECOM, SophiaTech Campus, 450 route des Chappes, 06904 Biot, France {jerome.haerri,dirk.slock}@eurecom.fr

¹To remain technology neutral, a “Beacon” is a message periodically broadcast by each node.

²CAM and ITS-G5 are European counterparts to the Basic Safety Message (BSM) and Dedicated Short Range Communication (DSRC) in the US. ITS-G5 is expected to be available in every vehicle sold from 2019.

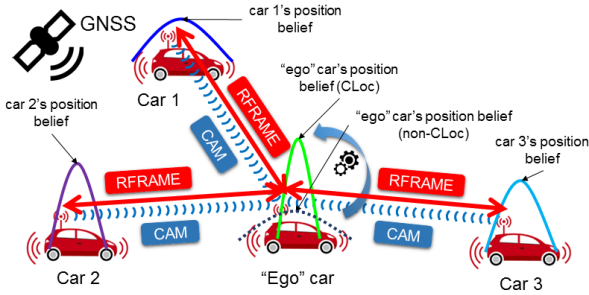


Fig. 1. “Ego” car receiving CAMs and exchanging ranging frames RFRAME from/with single-hop “virtual anchors” to perform distributed CLoc. The CLoc positional beliefs (i.e., through GNSS/IMU/WSS/V2V or IMU/WSS/V2V) are expected to be more concentrated than that of non-CLoc (i.e., with either GNSS/IMU/WSS or IMU/WSS).

V2V and V2I capabilities for better robustness. The latter solution claims good suitability in pathological environments under GNSS full blockage conditions such as long tunnels. The main contributions of the paper include: (i) describing the proposed Bayesian data fusion framework relying on Particle Filtering (PF), which combines IMU/WSS-based position predictions with both V2V and V2I range-dependent measurements; (ii) examining the localization potential of two kinds of V2I modalities and technologies (i.e., IR-UWB ToF-based ranges vs. ITS-G5 RSSIs), in terms of achievable performance trade-offs between accuracy gains (i.e., capability to mitigate divergence effects in GNSS-free CLoc) and cost (in consideration of the deployed extra-infrastructure); and finally, (iii) comparing the previous strategies with solutions based on GNSS repeaters and/or on a lane boundary detector (e.g., camera-based) that enables to spatially constrain the *posterior* density of location estimates.

The paper is organized as follows. Section II describes general concepts and system models related to vehicular CLoc, while Section III presents our new PF-based data fusion solution, capable of mixing V2V and V2I measurements. Simulation results and benchmarks are presented in Section IV. Finally, Section V concludes the paper and discloses planned future works.

II. PROBLEM STATEMENT AND SYSTEM MODEL

We consider a VANET consisting of a fleet \mathcal{V} of connected vehicles. At each vehicle $i \in \mathcal{V}$, time is locally sampled into a sequence of discrete events $t_{i,0}, t_{i,1}, \dots, t_{i,k}$, which are simply indexed by k^3 . Vehicles’ dynamic states are defined by $\mathbf{X}_{i,k}$, $i \in \mathcal{V}$ collecting components of interest e.g., the 2-D *absolute* position $\mathbf{x}_{i,k} = (x_{i,k}, y_{i,k})^\dagger$, the 2-D velocity $\mathbf{v}_{i,k} = (v_{i,k}^x, v_{i,k}^y)^\dagger$, the heading $\theta_{i,k}$, etc. **Note that $(\cdot)^\dagger$ is the transpose of its argument.** These state variables are assumed to evolve according to an *a priori* mobility model. At local discrete time k , the “ego” vehicle i has the set $\mathcal{S}_{\rightarrow i,k}$, $i \notin \mathcal{S}_{\rightarrow i,k}$ of “virtual anchors”, the set $\mathcal{T}_{\rightarrow i,k}$ of fixed anchors (i.e., static RoadSide Units (RSUs)), and acquires an observation vector $\mathbf{z}_{i,k}$, which is related to its own state $\mathbf{X}_{i,k}$,

³Due to asynchronously sampled time instants, the index k is locally meaningful. For notation brevity, the subscript indicating the vehicle index is dropped. If, however, it is included, the associated variable is strictly considered w.r.t. the timeline of the stated vehicle index.

its neighboring states \mathbf{X}_{j,k_i} , $j \in \mathcal{S}_{\rightarrow i,k}$, and its connected RSUs’ positions $\mathbf{X}_{l,k_i} = \mathbf{x}_l$, $l \in \mathcal{T}_{\rightarrow i,k}$ via a measurement model.

A. True Mobility and Mobility Prediction Models Mismatch

We herein assume a Gauss-Markov mobility model, which well describes the correlated velocity of vehicles in the form of a time-correlated Gauss-Markovian process suitable into vehicular contexts [4], as follows

$$\underbrace{\begin{pmatrix} \mathbf{x}_{i,k+1} \\ \mathbf{v}_{i,k+1} \end{pmatrix}}_{\mathbf{X}_{i,k+1}} = \begin{pmatrix} \mathbf{I}_2 & \alpha \Delta T \mathbf{I}_2 \\ \mathbf{0}_2 & \alpha \mathbf{I}_2 \end{pmatrix} \underbrace{\begin{pmatrix} \mathbf{x}_{i,k} \\ \mathbf{v}_{i,k} \end{pmatrix}}_{\mathbf{X}_{i,k}} + (1 - \alpha) \begin{pmatrix} \Delta T \mathbf{I}_2 \\ \mathbf{I}_2 \end{pmatrix} \bar{\mathbf{v}}_i + \sqrt{1 - \alpha^2} \begin{pmatrix} 1/2 \Delta T^2 \mathbf{I}_2 \\ \Delta T \mathbf{I}_2 \end{pmatrix} \mathbf{w}_{i,k}, \quad (1)$$

where α is the memory level, ΔT the time step, $\bar{\mathbf{v}}_i = (\bar{v}_i^x, \bar{v}_i^y)^\dagger$ the 2-D asymptotic (cursing) velocity, $\mathbf{w}_{i,k} = (w_{i,k}^x, w_{i,k}^y)^\dagger \sim \mathcal{N}((0, 0)^\dagger, \mathbf{Q}_{i,k})$ the 2-D Gaussian noise term associated with noisy control inputs, $\mathbf{Q}_{i,k}$ the **noise covariance matrix**, and \mathbf{I}_2 the identity matrix of size 2×2 .

Although one can assume that each vehicle knows its own mobility model i.e., a model like in (1) or more generally, a conditional transition probability density function (pdf) $p(\mathbf{X}_{i,k+1} | \mathbf{X}_{i,k})$ (known *a priori* for highly controlled mobility regimes or possibly self-calibrated on the fly based on previous state estimates), this perception is usually an approximation of the true mobility statistics. To remain mobility-independent, the well-known kinematic bicycle model is employed as mobility prediction model [10], as follows

$$x_{i,k+1} \approx x_{i,k} + \Delta T s_{i,k} \cos(\theta_{i,k} + 1/2 \Delta T \omega_{i,k}), \quad (2a)$$

$$y_{i,k+1} \approx y_{i,k} + \Delta T s_{i,k} \sin(\theta_{i,k} + 1/2 \Delta T \omega_{i,k}), \quad (2b)$$

$$\theta_{i,k+1} = \theta_{i,k} + \Delta T \omega_{i,k}, \quad (2c)$$

where $\omega_{i,k}$ is the yaw rate and $s_{i,k}$ the speed. These signals are considered as driving inputs to the mobility prediction model. They can be provided by the gyroscope in the IMU and the WSS respectively. Defining the new state as $\mathbf{X}_{i,k} = (x_{i,k}, y_{i,k}, \theta_{i,k})^\dagger$ and the motion measurement as $\mathbf{u}_{i,k} = (s_{i,k}, \omega_{i,k})^\dagger$, the model in (2) can now be represented in a more compact form by a function $\mathbf{f}(\cdot)$, as follows

$$\mathbf{X}_{i,k+1} = \mathbf{f}(\mathbf{X}_{i,k}, \mathbf{u}_{i,k}). \quad (3)$$

Assuming the measurements $s_{i,k}$ and $\omega_{i,k}$ are independent of each other and Gaussian with variances $(\sigma_i^s)^2$ and $(\sigma_i^\omega)^2$ respectively, $\mathbf{u}_{i,k}$ is a 2-D Gaussian vector with covariance matrix

$$\Sigma_{i,k}^{\mathbf{u}} = \begin{pmatrix} (\sigma_i^s)^2 & 0 \\ 0 & (\sigma_i^\omega)^2 \end{pmatrix}. \quad (4)$$

B. Observation Models

1) *IR-UWB V2X Ranges*: Through a ranging protocol (e.g., based on the ToF estimation of transmitted packets involved in multiple-way handshake transactions [9], [11]), vehicle i at time $t_{i,k}$ estimates the V2X distance $z_{j \rightarrow i,k}$ to node j , $j \in \mathcal{S}_{\rightarrow i,k} \cup \mathcal{T}_{\rightarrow i,k}$ in position \mathbf{x}_{j,k_i} (or \mathbf{x}_j)

$$z_{j \rightarrow i,k} = \|\mathbf{x}_{i,k} - \mathbf{x}_{j,k_i}\| + n_{j \rightarrow i,k}, \quad (5)$$

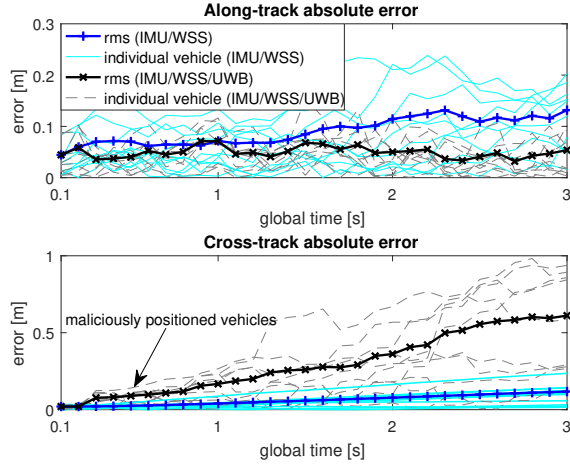


Fig. 2. $1\text{-}\sigma$ along-track (top) and cross-track (bottom) errors perceived by fusion filters for each vehicle during the first 3 seconds for non-CLoc (IMU/WSS) and pure CLoc (IMU/WSS/UWB). Simulation settings and scenarios are given in Sec. IV-A.

where $n_{j \rightarrow i,k} \sim \mathcal{N}(0, \sigma_{\text{UWB}}^2)$ is the ranging measurement noise of standard deviation σ_{UWB} .

Note that node j could be indifferently another mobile “virtual anchor” or a static RSU set as fixed anchor (i.e., a true anchor).

2) *V2X Received Power*: Out of a received CAM, the RSSI $z_{j \rightarrow i,k}$ (on a dB scale) measured by vehicle i at time $t_{i,k}$ with respect to vehicle j , $j \in \mathcal{S}_{\rightarrow i,k} \cup \mathcal{T}_{\rightarrow i,k}$ in position \mathbf{x}_{j,k_i} (or \mathbf{x}_j) is assumed to follow the widely used log-distance path loss model

$$z_{j \rightarrow i,k} = P(d_0) - 10n_p \log_{10}(\|\mathbf{x}_{i,k} - \mathbf{x}_{j,k_i}\|) + X_{j \rightarrow i,k}, \quad (6)$$

where $P(d_0)$ [dBm] is the average received power at a reference distance d_0 , n_p the path loss exponent, $X_{j \rightarrow i,k} \sim \mathcal{N}(0, \sigma_{\text{Sh}}^2)$, and σ_{Sh} the shadowing standard deviation.

Similarly to IR-UWB ToF-based range measurements, node j is herein either a “virtual anchor” or a true anchor.

3) *GNSS Repeater-Based Absolute Position*: The 2-D position estimate delivered by a GNSS receiver, $\mathbf{p}_{i,k} = (p_{i,k}^x, p_{i,k}^y)^\dagger$, is affected by an Additive White Gaussian Noise (AWGN) vector $\mathbf{n}_{i,k} = (n_{i,k}^x, n_{i,k}^y)^\dagger \sim \mathcal{N}((0,0)^\dagger, \sigma_{\text{GNSS}}^2 \mathbf{I}_2)$ [2], [4] of standard deviation σ_{GNSS} .

$$p_{i,k}^x = x_{i,k} + n_{i,k}^x, \quad p_{i,k}^y = y_{i,k} + n_{i,k}^y. \quad (7)$$

Finally, for the sake of notation brevity and simplicity, we introduce the following set notation to gather different vehicles’ variables: stacked state of “virtual anchors” $\mathbf{X}_{\mathcal{S} \rightarrow i,k} = \{\mathbf{x}_{j,k_i} | \forall j \in \mathcal{S}_{\rightarrow i,k}\}$ and $\mathbf{X}_{\mathcal{S} \rightarrow i,k^-} = \{\mathbf{x}_{j,k < k_i} | \forall j \in \mathcal{S}_{\rightarrow i,k}\}$; stacked state of fixed anchors in range $\mathbf{X}_{\mathcal{T} \rightarrow i,k} = \{\mathbf{x}_j | \forall j \in \mathcal{T}_{\rightarrow i,k}\}$; full stacked state $\mathbf{X}_{i,\text{USUT},k} = (\mathbf{X}_{i,k}^\dagger, \mathbf{X}_{\mathcal{S} \rightarrow i,k}^\dagger, \mathbf{X}_{\mathcal{T} \rightarrow i,k}^\dagger)^\dagger$; V2V measurement vector $\mathbf{z}_{\mathcal{S} \rightarrow i,k} = \{z_{j \rightarrow i,k} | \forall j \in \mathcal{S}_{\rightarrow i,k}\}$; and V2I measurement vector $\mathbf{z}_{\mathcal{T} \rightarrow i,k} = \{z_{j \rightarrow i,k} | \forall j \in \mathcal{T}_{\rightarrow i,k}\}$.

C. Divergence of Position Estimates and Errors Propagation

In a pure VANET context, the performance of range-based CLoc depends on three critical factors: (i) the quality of

range measurements, (ii) the uncertainty of prior position estimates for both the “ego” vehicle and “virtual anchors”, and (iii) the local geometric configuration of the latter anchors relatively to the “ego” vehicle (i.e., GDoP conditions). The first condition can be satisfied by choosing an accurate time-based ranging technology such as IR-UWB. However, despite fine V2V ranging accuracy, as the position estimated through CLoc at each “ego” vehicle depends on the previous estimate (via the IMU/WSS-based position prediction) and on the neighbors’ estimates (via cooperation), errors tend to accumulated over both time and space. Estimation is then subject to significant unbounded biases unless absolute re-calibration is performed or much better GDoP is achieved. Unfortunately, none of these conditions is usually met in standard tunnels. Since mobility is strongly constrained by the roads/lanes and driving rules, the vehicles’ relative geometry is rather poorly conditioned in this context. More particularly, the VANET topology is usually distorted along the direction colinear to the road due to the huge disparity between the longitudinal safety distances (e.g., 20–150 m⁴) and the lateral lane width (e.g., 2.25–3.5 m). Accordingly, the GDoP is likely poor in the direction orthogonal to the road; therefore, the cross-track location error remains high. Such situations can be fatal, since such malicious information cannot be re-calibrated by absolute means and then is propagated over the network and degrades the position accuracy of all neighbors accordingly. Fig. 2 illustrates this phenomenon where CLoc uniquely based on V2V IR-UWB measurements yields worse accuracy than IMU/WSS non-CLoc. Fig. 2(a) confirms the advantage of CLoc to decrease the along-track error whereas Fig. 2(b) shows that jointly or separately, poor GDoP effects and neighbors’ unbounded biased position estimates lead to the faster divergence of CLoc accuracy along the cross-track direction (which dominates the total localization error) in comparison with non-CLoc.

III. PROPOSED DATA FUSION FRAMEWORK

A. Distributed PF for Hybrid CLoc based on V2X

PF is attractive for nonlinear sequential state estimation when KF-based methods may diverge. Moreover, PF is intrinsically nonparametric with respect to the posterior density, which may be arbitrarily complex and multimodal. In PF, the latter density, $p(\mathbf{X}_{i,k} | \mathbf{z}_{i,1:k})$, is approximated by a particles cloud of P random samples $\{\mathbf{X}_{i,k}^{(p)}\}_{p=1}^P$ with associated weights $\{w_{i,k}^{(p)}\}_{p=1}^P$ [10] i.e., $p(\mathbf{X}_{i,k} | \mathbf{z}_{i,1:k}) \approx \sum_{p=1}^P w_{i,k}^{(p)} \delta(\mathbf{X}_{i,k} - \mathbf{X}_{i,k}^{(p)})$, where $\delta(\cdot)$ is the Dirac delta function. However, it is challenging and expensive from a computational point of view to draw samples directly from $p(\mathbf{X}_{i,k} | \mathbf{z}_{i,1:k})$ due to its complex functional form [10]. Thus, an approximate distribution called the sequential proposal density $\pi(\mathbf{X}_{i,k}, \mathbf{X}_{\mathcal{S} \rightarrow i,k} | \mathbf{X}_{i,k-1}^{(p)}, \mathbf{X}_{\mathcal{S} \rightarrow i,k-1}^{(p)}, \mathbf{z}_{i,1:k})$ is used instead, from which one can easily draw samples. One popular embodiment thus consists in using the mobility model as the

⁴The two-second (or three-second) rule is applied to maintain a safe following distance.

Algorithm 1 Bootstrap PF (iteration k , “ego” vehicle i)

- 1: **CAM Collection:** Receive CAMs from the set $\mathcal{N}_{\rightarrow i,k}$ of perceived neighbors, exact the parametric beliefs, and draw samples to reconstruct the approximated particle clouds $\{\tilde{\mathbf{X}}_{i,k}^{(p)}, 1/P\}_{p=1}^P, j \in \mathcal{N}_{\rightarrow i,k}$.
- 2: **Data Resynchronization:** Perform prediction of both “ego” and neighboring particle clouds based on mobility models in (3) at time $t_{i,k}$

$$\begin{aligned} \mathbf{X}_{i,k}^{(p)} &\sim p(\mathbf{X}_{i,k} | \mathbf{X}_{i,k-1}^{(p)}), \quad p = 1, \dots, P, \\ \mathbf{X}_{j,k_i}^{(p)} &\sim p(\mathbf{X}_{j,k_i} | \tilde{\mathbf{X}}_{j,k}^{(p)}), \quad p = 1, \dots, P, \quad j \in \mathcal{N}_{\rightarrow i,k}. \end{aligned}$$

- 3: **Observation Query and Aggregation:** Select the subset $\mathcal{S}_{\rightarrow i,k} \subset \mathcal{N}_{\rightarrow i,k}$ of paired “virtual anchors” and the set $\mathcal{T}_{\rightarrow i,k}$ of paired true anchors. Aggregate the measurements (and the corresponding observation model) $\mathbf{z}_{i,k} = (\mathbf{z}_{\mathcal{S}_{\rightarrow i,k}}^\dagger, \mathbf{z}_{\mathcal{T}_{\rightarrow i,k}}^\dagger)^\dagger$.
- 4: **Correction:** Calculate the new weights according to the likelihood

$$\begin{aligned} w_{i,k}^{(p)} &\propto p(\mathbf{z}_{i,k} | \mathbf{X}_{i \cup \mathcal{S} \cup \mathcal{T}, k}^{(p)}) = \prod_{j \in \mathcal{S}_{\rightarrow i,k}} p(z_{j \rightarrow i,k} | \mathbf{X}_{j,k_i}^{(p)}, \mathbf{X}_{i,k}^{(p)}) \times \\ &\quad \prod_{l \in \mathcal{T}_{\rightarrow i,k}} p(z_{l \rightarrow i,k} | \mathbf{x}_l, \mathbf{X}_{i,k}^{(p)}), \quad p = 1, \dots, P, \end{aligned}$$

normalize them to sum to unity, and compute the approximate Minimum Mean Square Error (MMSE) estimator as the second filter/fusion output $\hat{\mathbf{X}}_{i,k} \approx \sum_{p=1}^P w_{i,k}^{(p)} \mathbf{X}_{i,k}^{(p)}$.

- 5: **Resampling, Message Approximation, Broadcast**

sequential proposal density [1], [10] i.e.,

$$\boldsymbol{\pi}(\cdot) = p(\mathbf{X}_{i,k} | \mathbf{X}_{i,k-1}^{(p)}) \prod_{j \in \mathcal{S}_{\rightarrow i,k}} p(\mathbf{X}_{j,k_i} | \mathbf{X}_{j,k}^{(p)}). \quad (8)$$

Note that the above function describes a joint mobility model of both “ego” and neighboring vehicles. Therefore, the drawn samples take into account the uncertainty of “virtual anchors”. This step is particularly crucial. Indeed, if the PF treated “virtual anchors” as real anchors, more estimation biases affecting the neighboring estimates would be propagated to the “ego” vehicle, leading to even more significant accuracy degradation.

Then we propose to apply this filter as the core fusion engine in our CLoc framework, as described in Algorithm 1 (including also side CAM reception, message approximation and CAM broadcast steps). Note that our PF-based data fusion combines the V2X measurements to give robust and accurate position estimates in Step 3 and 4.

B. Deployment of GNSS Repeaters

Another infrastructure-based solution to assist CLoc with absolute positioning capabilities consists in deploying GNSS repeaters in tunnels instead of RSUs. From the localization point of view, the Algorithm 1 is thus modified in Step 3 and Step 4 so as to integrate the GNSS observation. Accordingly, the measurement vector in Step 3 becomes $\mathbf{z}_{i,k} = (\mathbf{p}_{i,k}^\dagger, \mathbf{z}_{\mathcal{S}_{\rightarrow i,k}}^\dagger)^\dagger$ and the weights are now updated as follows $w_{i,k}^{(p)} \propto p(\mathbf{z}_{i,k} | \mathbf{X}_{i,k}^{(p)}, \mathbf{X}_{\mathcal{S}_{\rightarrow i,k}}^{(p)}) = p(\mathbf{p}_{i,k} | \mathbf{X}_{i,k}^{(p)}) \prod_{j \in \mathcal{S}_{\rightarrow i,k}} p(z_{j \rightarrow i,k} | \mathbf{X}_{j,k_i}^{(p)}, \mathbf{X}_{i,k}^{(p)})$, $p = 1, \dots, P$.

C. Integration of Lane Constraints (LCs)

The mobility of land vehicles is tightly constrained by the road and lane boundaries. Thus, such contextual information can be contributed into the localization problem [12]. We

TABLE I
MAIN SIMULATION PARAMETERS

Parameter	Value
Sampling period ΔT	0.1 [s] (<i>fast update rate for high mobility</i>)
Gyroscope signal noise	0.1 [deg/s] (rms) [13]
WSS noise	1% actual speed [13]
V2X IR-UWB ranging rate	5 [Hz] (V2V), 10 [Hz] (V2I)
V2X IR-UWB ranging noise	0.2 [m] (rms)
V2X IR-UWB communication range	600 [m]
V2X CAM rate	10 [Hz] (critical)
V2X CAM range	1000 [m] [6]
Path loss exponent n_p	1.6 (V2V in tunnels) [14]
Std. of shadowing σ_{sh}	3.4 [dB] (V2V in tunnels) [14]
Inter-site RSU interval	500, 200, and 100 [m]
GNSS rate	10 [Hz]
GNSS noise	1.5 [m] (SBAS ^a), 3.6 [m] (SPS ^b) (rms) [15]
GNSS repeater noise	5–10 [m] (rms)
Number of particles	1000
Initial pos. errors in x - and y -axes	1 [m] (rms) (plausible hypothesis)
Initial heading error	4 [deg] (rms) (plausible hypothesis)

^a Satellite-Based Augmentation System.

^b Standard Positioning Service.

assume in this paper that lane allocation can be performed at each vehicle using for instance a vision-based system (e.g., monocular camera) and a digital map [13]. The latest filtered/fused estimate is cross-checked with the side digital map to identify the current road occupancy and its associated attributes (e.g., lanes number and width). In addition, the camera system scans the road and detects the lanes [13] As a result, the absolute positions of the lane boundaries can be determined and used to constrain the filtered/fused outputs. In this method, the posterior density of location estimate is numerically truncated beyond the lane boundaries, which are considered as constraints to restrict the valid state domain. More precisely, particles lying outside a drivable area are removed. Finally, the constrained density is constructed based on the remaining valid samples on the occupied lane. This truncated density is subsequently used to calculate the filter MMSE output.

IV. PERFORMANCE EVALUATION

A. Simulation Settings and Scenarios

In our MATLAB-based evaluations, we consider a 1000-m three-lane straight tunnel, where 10 ITS-G5 connected vehicles endowed with IR-UWB ranging capabilities (V2V and/or V2I) are driving steadily in a common direction at the average speed of 70 km/h. In addition, RSUs are deployed along the tunnel, with different inter-site intervals of 500, 200, and 100 meters either on one single side of the road or on both sides as shown in Fig. 3. These units support both ITS-G5 and IR-UWB technologies for both V2I communication and V2I ranging w.r.t. mobile vehicles. The main simulation parameters are summarized in Table I.

B. Numerical Results

1) *Localization Performance Comparison:* The localization performance achieved for different algorithmic and technological options is summarized in Fig. 4 by means of empirical Cumulative Distribution Functions (CDFs). Dead

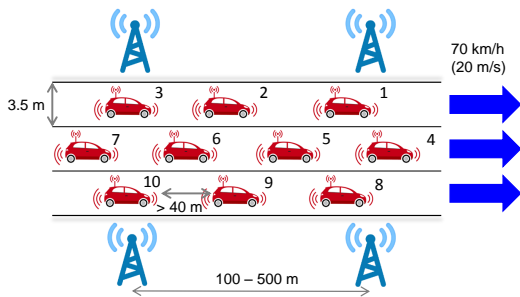


Fig. 3. Evaluated VANET and related attributes in 1000-m straight tunnel scenario.

Reckoning (DR) based on IMU and WSS is by default assumed available at each vehicle and thus considered in all the tested scenarios (either as standalone solution or in combination with other technologies).

Fig. 4(a) shows spectacular performance gains when using RSUs with accurate IR-UWB ranging capabilities even under reasonably loose deployments i.e., with inter-site RSUs intervals of 500 m on both sides of the tunnel. As aforementioned, conventional DR provides relatively poor performance in the long-term due to error accumulation and resulting drift effects, whereas pure ad hoc V2V cooperation based on both IR-UWB V2V measurements and DR (thus, relying on ill-positioned “virtual anchors”) leads to mutual contamination among vehicles and even worse localization performance in the end. The capability to provide CLoc with reliable *absolute* information however strongly depends on the V2I ranging technology available at RSUs. In particular, the addition of V2I range measurements based on IR-UWB yields significant performance gain over DR (relative drops of 88% in median error and 85% in worst-case (WC) error (defined for a CDF of 90%)) and pure ad hoc CLoc (relative drops of 94% and 90% in median and WC errors respectively), while V2I RSSI measurements based on ITS-G5 are not sufficiently informative so that the localization performance is equivalent to that of a pure ad hoc case relying on IR-UWB V2V ranging and DR. RSSI-based positioning is indeed usually not considered as a high precision solution [3], [9]. Thus its contribution to the position estimate correction (by updating the weights in Algorithm 1 in Step 4) is relatively marginal in comparison with that of accurate V2V IR-UWB ranges.

In Fig. 4(b), we compare the proposed RSU-based solution with the use of LC (with DR) or GNSS repeaters (with DR), assuming in the latter case systematic GNSS signal availability in the entire tunnel⁵ but various quality levels. It is indeed reasonable to assume degraded accuracy in comparison with open-sky conditions due to multi-path propagation (e.g., SPS and SBAS accuracy of 1.5 m and 3.6 m respectively [15]). It is thus observed that the *absolute* positional information provided by GNSS repeaters must be accurate enough to be able to re-calibrate position estimates. However, this information is always beneficial for fusion since it is assumed to be bounded and unbiased. Besides,

⁵This is usually achieved with typical inter-side intervals in the range of 30 – 50 m)

the non-CLoc scheme including LC and DR outperforms the solution based on GNSS repeaters but still cannot reach the performance level of full V2X CLoc including IR-UWB range measurements w.r.t. both mobile neighbors and RSUs, even if the performance gap is not so significant (increased median and WC errors of 12 cm and 8 cm respectively). Two main reasons can be invoked to explain this phenomenon. First, we have considered a very accurate WSS sensor in our validations [13]. LC naturally thus tends to correct the only remaining accumulated errors affecting the input heading measurements used in state predictions. Second, the tested RSU deployment (i.e., 500-m inter-site interval) is rather sparse, leading to an average number of 4 connected anchors (as shown in Fig. 5), what contributes to sustain poor GDoP conditions.

In Fig. 4(c), we are interested in more *aggressive* scenarios to boost localization accuracy. In particular, we assume a denser RSU deployment (e.g., down to 100-meter inter-site intervals) and more accurate GNSS repeaters reaching optimistically the open-sky accuracy of SPS or even SBAS. Let us now consider the non-CLoc scheme with LC and DR as a reference baseline. By using massive RSUs, the V2I RSSI now yields better performance and at least outperforms the standalone DR solution (relative decreases of 67% and 24% in median and WC errors respectively) but still cannot be compared with the proposed full CLoc scheme relying on both V2V and V2I IR-UWB range measurements.

Then, we verify *if* and *to which extent* it is possible to improve also the solution based on ITS-G5 V2I RSSI measurements by integrating LC. However, it only gives comparable performance levels with the solution combining DR and LC, due to inaccurate ITS-G5 V2I RSSIs again.

When assuming even more optimistic GNSS repeater accuracy to the level of open-sky in the exchange of increased cost of deployment, only the solution combining SBAS and DR yields performance gains over the solution combining LC and DR, even though yet the gap is not so remarkable. Under denser IR-UWB RSUs deployment, much better accuracy is achievable through full V2X CLoc (relative drops of 68% and 60% in median and WC errors respectively w.r.t. the DR and LC).

2) *Deployment Cost Analysis and Discussion:* We confront here the trade-off between the accuracy gain and the associated deployment cost. Particularly, we compare the use of IR-UWB RSUs and GNSS repeaters for tunnels. We claim that the IR-UWB RSU approach is more favorable than the GNSS repeater scheme in terms of both accuracy performance and deployment cost. As an illustration, in the considered 1000-meter tunnel scenario, we would need to place about 20–35 repeaters (i.e., one every 30–50 meters) to achieve the accuracy of 0.4–2 m whereas 6–20 IR-UWB RSUs yield 0.2–0.1 m⁶. Motivated by the clear benefits from RSUs, we further compare different RSU configurations, as depicted in Fig. 5. A closer look at the figure reveals

⁶We assume in first approximation that the deployment efforts -and thus costs/unit- of GNSS repeaters and IR-UWB RSUs are comparable.

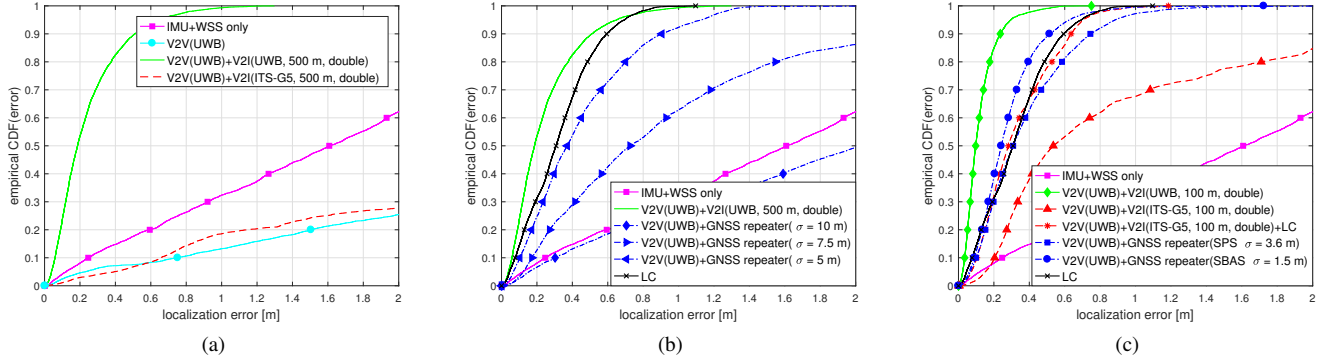


Fig. 4. Empirical CDF of localization errors for different filter/fusion schemes. Note that all the options implement IMU/WSS-based position prediction.

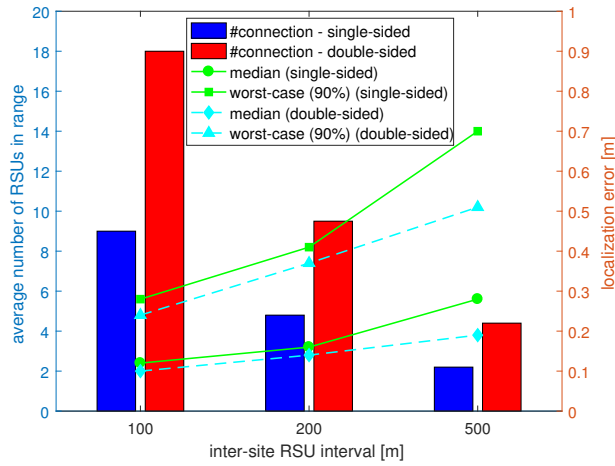


Fig. 5. Impact of the RSU deployment on V2X UWB CLoc's loc. accuracy.

that with a similar number of connected RSUs (as well as a total number of deployed RSUs) (e.g., single-sided 200-meter inter-site RSUs interval vs. double-sided 500-meter and double-sided 200-meter vs. single-sided 100-meter), the shorter inter-site RSUs interval, the better accuracy. It is due to the fact that cross-track error is significantly reduced when vehicles pass by the anchors (See [16] for more details). Thus, short inter-site RSUs interval shall be preferred to looser double-sided deployment.

V. CONCLUSION AND FUTURE WORKS

We investigate the problem of range-based CLoc for VANETs specifically in tunnel environments. Simulation results clearly indicate that in long tunnels, CLoc only with respect to neighboring vehicles is prone to fast divergence and inaccurate position estimates. We solve this problem by additionally integrating V2I measurements with respect to RSUs, which are deployed along the tunnel, relying on an adapted PF-based data fusion framework. By applying the proposed hybrid CLoc with generalized V2X measurements (i.e., V2I on top of V2V), we have found that: (i) V2I IR-UWB range measurements boost the CLoc accuracy even under sparse RSUs deployment; (ii) V2I RSSI only slightly improves the CLoc accuracy in case of massive RSUs deployment; (iii) V2X IR-UWB CLoc is more attractive

than the CLoc assisted by GNSS repeaters in terms of both accuracy performance and cost of deployment. Future works will study communication aspects (e.g., efficient protocol design for packet exchanges, impact of packet error rate, etc.) on the localization performance.

REFERENCES

- [1] G. M. Hoang, B. Denis, J. Härrä, and D. T. M. Slock, "Breaking the gridlock of spatial correlations in GPS-aided IEEE 802.11p-based cooperative positioning," *IEEE Trans. on Veh. Technol.*, vol. 65, pp. 9554–9569, Dec. 2016.
- [2] N. Drawil and O. Basir, "Intervehicle-communication-assisted localization," *IEEE Trans. on Intel. Transp. Syst.*, vol. 11, pp. 678–691, Sept. 2010.
- [3] R. Parker and S. Valaee, "Vehicular node localization using received-signal-strength indicator," *IEEE Trans. on Veh. Technol.*, vol. 56, pp. 3371–3380, Nov. 2007.
- [4] G. M. Hoang, B. Denis, J. Härrä, and D. T. M. Slock, "Select thy neighbors: Low complexity link selection for high precision cooperative vehicular localization," in *Proc. VNC'15*, pp. 36–43, Dec. 2015.
- [5] J. Liu, B. g. Cai, and J. Wang, "Cooperative localization of connected vehicles: Integrating GNSS with DSRC using a robust cubature Kalman filter," *IEEE Trans. on Intel. Transp. Syst.*, vol. PP, pp. 1–15, Dec. 2016.
- [6] "Intelligent Transport Systems (ITS); Vehicular Communications; Basic Set of Applications; Part 2: Specification of Cooperative Awareness Basic Service," *ETSI Std. EN 302 637-2 V1.3.2*, Oct. 2014.
- [7] G. M. Hoang, B. Denis, J. Härrä, and D. T. M. Slock, "Cooperative localization in GNSS-aided VANETs with accurate IR-UWB range measurements," in *Proc. WPNC'16*, Oct. 2016.
- [8] M. G. Petovello *et al.*, "Demonstration of inter-vehicle UWB ranging to augment DGPS for improved relative positioning," in *Proc. ION GNSS'10*, pp. 1198–1209, Sep. 2010.
- [9] Z. Sahinoglu, S. Gezici, and I. Gvenc, *Ultra-wideband Positioning Systems: Theoretical Limits, Ranging Algorithms, and Protocols*. New York, NY, USA: Cambridge University Press, 2011.
- [10] S. Thrun, W. Burgard, and D. Fox, *Probabilistic Robotics (Intelligent Robotics and Autonomous Agents)*. The MIT Press, 2005.
- [11] M. Maman, B. Denis, M. Pezzin, B. Piaget, and L. Ouvry, "Synergetic MAC and higher layers functionalities for UWB LDR-LT wireless networks," in *Proc. ICUWB'08*, vol. 3, pp. 101–104, Sept. 2008.
- [12] P. Groves, *Principles of GNSS, Inertial, and Multisensor Integrated Navigation Systems*. Boston-London, UK: Artech House, 2nd ed., 2013.
- [13] "D5.2 - Specifications of implemented cooperative and fusion algorithms," *HIGHTS Deliverable*, Aug. 2016.
- [14] J. Kunisch and J. Pamp, "Wideband car-to-car radio channel measurements and model at 5.9 GHz," in *Proc. VTC'08-Fall*, Sept. 2008.
- [15] USDOD and NAVSTAR GPS, *GPS Standard Positioning Service (SPS) Performance Standard*, 4th ed., Sep. 2008.
- [16] G. M. Hoang, B. Denis, J. Härrä, and D. T. M. Slock, "Mitigating unbalanced GDoP effects in range-based vehicular cooperative localization," in *Proc. ICC-ANLN*, May 2017. to appear.